https://doi.org/10.5194/angeo-2023-37
Preprint. Discussion started: 4 January 2024

Annales Geophysicae Discussions
Open Access
EGU

Ionospheric Upwelling and the Level of Associated Noise at Solar Minimum

Timothy Wemimo David[1,2], Chizurumoke Michael Michael[3,2], Darren Wright[2], Adetoro Temitope Talabi[1], and Abayomi Ekundayo Ajetunmobi[1]

[1]Department of Physics, Olabisi Onabanjo University, Ago-Iwoye, Nigeria
[2]Department of Physics and Astronomy, University of Leicester, Leicester, UK
[3]Faculty of Arts, Science and Technology (FAST), University of Northampton, Northampton, UK

Correspondence: Chizurumoke Michael Michael (michael.michael@northampton.ac.uk)

Abstract. We have studied the ionospheric upwelling with magnitude above $10^{13}m^{-2}s^{-1}$ using the data during the IPY-ESR 2007 campaign, which coincides with solar minimum. The noise level in low, medium and high-flux upflows is investigated. We found that the noise level in high-flux upflow is about 93% while the low and medium categories are 62% and 80%, respectively. This shows that robust and stringent filtering techniques must be ensured when analysing incoherent data in order not to bias the result. Analysis reveals that the frequency of the low-flux upflow events is about 8 and 73 times the medium and high-flux upflow events, respectively. Seasonal observation shows that the noise level in the upflow classes is predominantly during winter. The noise is minimal in summer, with a notable result indicating occurrence of actual data above noise in the low-flux class. Moreover, the percentage occurrence of the noise level in the data increases with increasing flux strength, irrespective of the season. Further analysis reveals that the noise level in the local time variation peaked around 17 – 18 LT and minimum around local noon.

1 Introduction and Instrumentation

The European Incoherent Scatter Scientific Association (EISCAT, Rishbeth, 1985) an international scientific body set up to carry out research, using the Incoherent Scatter Radar (ISR) technique to probe the ionosphere as well as the different layers of the atmosphere (Fu et al., 2015). The electromagnetic pulses transmitted from the radar interact with the ionospheric plasma, and the latter emits a fractional part of the exploring signal as scattering. The backscatter frequency spectrum received (referred to as the incoherent scatter (IS) spectrum) provides various information on properties and state of the ionosphere (Rishbeth and Williams, 1985). Several key ionospheric parameters can be derived from the IS spectrum (e.g., Gordon, 1958; Dougherty and Farley, 1961; Evans, 1969; Alcayde, 1997; Li et al., 2012). Such parameters include the electron density, ion and electron temperature, and the ion drift velocity relative to the radar.

The data from ISR have been previously analysed by several authors. For example, Ogawa et al. (2009) used the ISR data to show that ionospheric upwelling can occur at any local time (LT). Vlasov et al. (2011), while analysing the EISCAT data of international polar year (IPY) 2007 have shown that travelling ionospheric disturbances and atmospheric gravity waves are common high latitudes phenomena, frequent during summer. More recently, David et al. (2018), using the same set of data,

https://doi.org/10.5194/angeo-2023-37
Preprint. Discussion started: 4 January 2024

Annales Geophysicae Discussions

have shown that the maximum occurrence peak of ion upwelling, irrespective of the class, occurs around local noon. Such analysis of data from Tromsø, where EISCAT VHF radar operates, shows that ionospheric upflow and downflow are possible under any level of geomagnetic condition (Endo et al., 2000). According to Foster et al. (1998) in their study of some of the EISCAT frequently run programmes, occurrence frequency of upwelling ions has a direct relationship with altitudinal increase. The study of stimulated electromagnetic emission by EISCAT heating facility at Tromsø, used to modulate the ionosphere for experimental purposes, has shown that reduction is observed in the elevated electron temperature when the radio pumping is close to the gyro-harmonic frequency of the electron (Fu et al., 2015). Williams (1995) in his analysis of the initial phase of the EISCAT Svalbard Radar (ESR) observation proposed that to properly investigate the polar ionosphere dynamics, a facility that will address the **k** vector at a time (3-antenna facility) should be considered instead of the usual method of a single antenna swinging through the $x-$, $y-$ and $z-$directions in sequence. Although the ESR facility like other IS radars is built with high gain and low noise performance owing to its transmitted power (up to a maximum of 1.0 MW), antenna sensitivity (42 m diameter) and high latitude location $(78^{\circ}09^{'}11^{''}N)$, there are noise from other sources such as the signal-to-noise ratio (SNR) that varies inversely as the square of the distance from the receiver to the target (i.e.,$S \approx R^{-2}$), noise associated with clutter in altitude up to 140 km (Wannberg et al., 1997) and the electromagnetic noise at the background.

The data analysed in this work were observed by the EISCAT Svalbard Radar (ESR) 42 m dish between the altitude range of 100 and 470 km with a time resolution of 1 minute. The main focus of this paper is the analysis of noise associated with different classes of ionospheric upflow and seasonal variability of the noise during ESR observations of upwelling ions at solar minimum of 2007 – 2008 shown in Figure 1, where the maximum daily total sunspot number is 66.0 in 2007 and 60.0 in 2008. Likewise, the maximum daily F10.7 radio flux over the same period as shown in Figure 1 is 93.9 and 88.6 in 2007 and 2008 respectively. Noise or rejected data in this study refers to ISR data with very high values of unphysical velocities above 10 km s^{-1} unintentionally obtained during incoherent scatter analysis (Jones et al., 1988; Winser et al., 1988; Wahlund and Opgenoorth, 1989; Blelly et al., 1996; Ogawa et al., 2009; Skjæveland et al., 2014; David et al., 2018; Takada et al., 2021). The classes of flux in this study and the filtering methodology follow the work by David et al. (2018), where upflows are categorised as follows:

- Low-flux upflow, $1.0 \times 10^{13} m^{-2} s^{-1} \leq f_{ion} < 2.5 \times 10^{13} m^{-2} s^{-1}]$
- Medium-flux upflow, $2.5 \times 10^{13} m^{-2} s^{-1} \leq f_{ion} < 7.5 \times 10^{13} m^{-2} s^{-1}$
- High-flux upflow, $f_{ion} \geq 7.5 \times 10^{13} m^{-2} s^{-1}$

2 Results and Discussion

Figures 2 and 3 show the EISCAT Svalbard Radar ionospheric parameters plot for a dayside plot on August 12, 2007 and a nightside plot on December 28, 2007 respectively. The dayside plot in August 12, 2007 shows when the data is less noisy, while the nightside event represents a typical example of periods when ISR data is enmeshed with random unwanted data without physical meaning. The panels (a) to (e) on both figures are respectively the electron density, electron temperature, ion temper-

https://doi.org/10.5194/angeo-2023-37
Preprint. Discussion started: 4 January 2024

Annales Geophysicae Discussions
Open Access
EGU

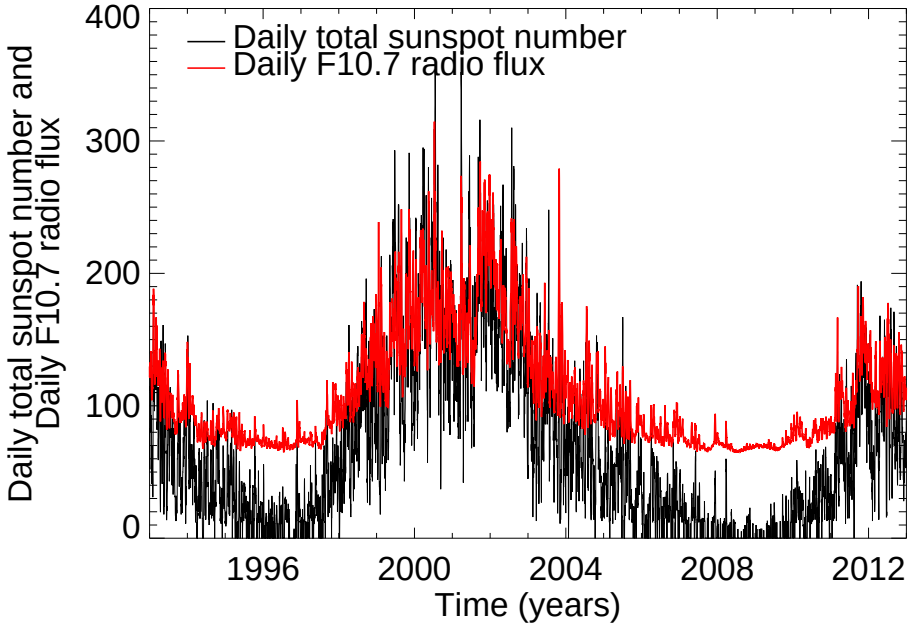

Figure 1. Daily sunspot number indicated by black and daily F10.7 radio flux indicated by red line adapted from David et al. (2018).

ature, ion drift velocity, and the ion flux. August 12, 2007 plot indicates intermittent moderately intense electron precipitation down to the E region from 06:00 UT to around 10:30 UT, and thereafter remains predominantly moderate throughout the rest of the period. On the other hand, the nightside event of December 28, 2007 shows that the ionosphere was predominantly quiet with little or no electron precipitation to the E region, expect for the evening time. The F region electron density in Figure 2 indicates a long duration of elevation whereas, the F region electron density did not record significant enhancement in Figure 3. On the second topmost panel is the electron temperature, which indicates corresponding enhancement to the period of precipitation during the August 12, 2007 event shown in Figure 2, while the same panel on Figure 3 shows a noisy period especially at the lower and higher altitude. The middle panel indicates that a moderate with few intermittent intense ion temperature dominate the period on August 12, 2007 event. The period between 22:00UT on December 28, 2007 and 02:00 UT the following day, indicates a mixture of moderate and elevated ion temperature. Panels d and e on Figure 2 show accelerated ions around afternoon and a corresponding high-flux respectively, whereas the ion velocity in Figure 3 are unphysical and there is no corresponding high-flux upflow.

Table 1 shows the number of data points for both unfiltered and actual (filtered) data for each class of ion upflow flux, as well as the percentages of the actual and noisy data. The actual data is the number of data points that satisfy the filtering technique

https://doi.org/10.5194/angeo-2023-37
Preprint. Discussion started: 4 January 2024

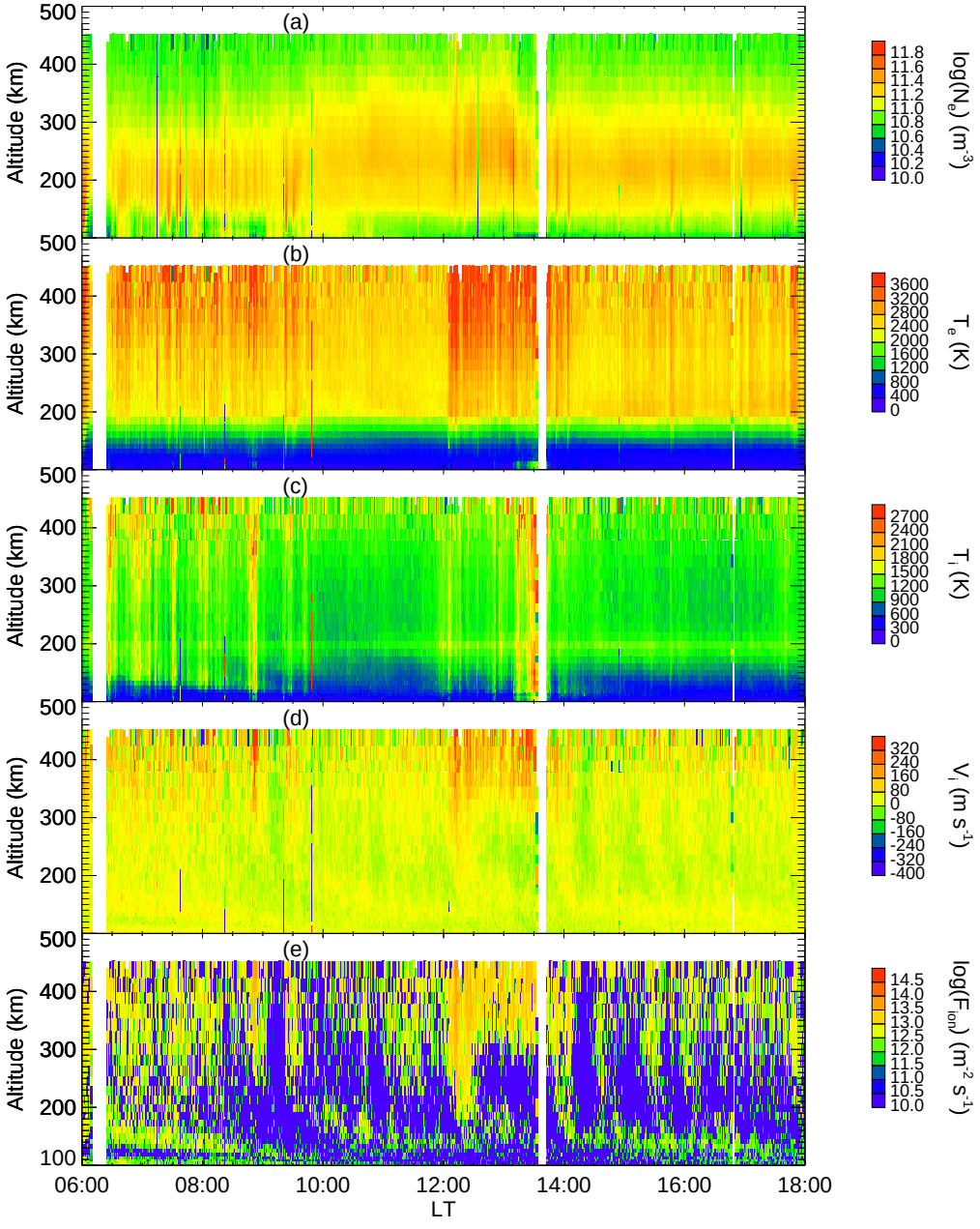

Figure 2. EISCAT Svalbard Radar (42 m dish) parameter plot for dayside 11 September, 2007. The panels a – e are respectively the electron density, electron temperature, ion temperature, ion drift velocity and the ion flux.

https://doi.org/10.5194/angeo-2023-37
Preprint. Discussion started: 4 January 2024

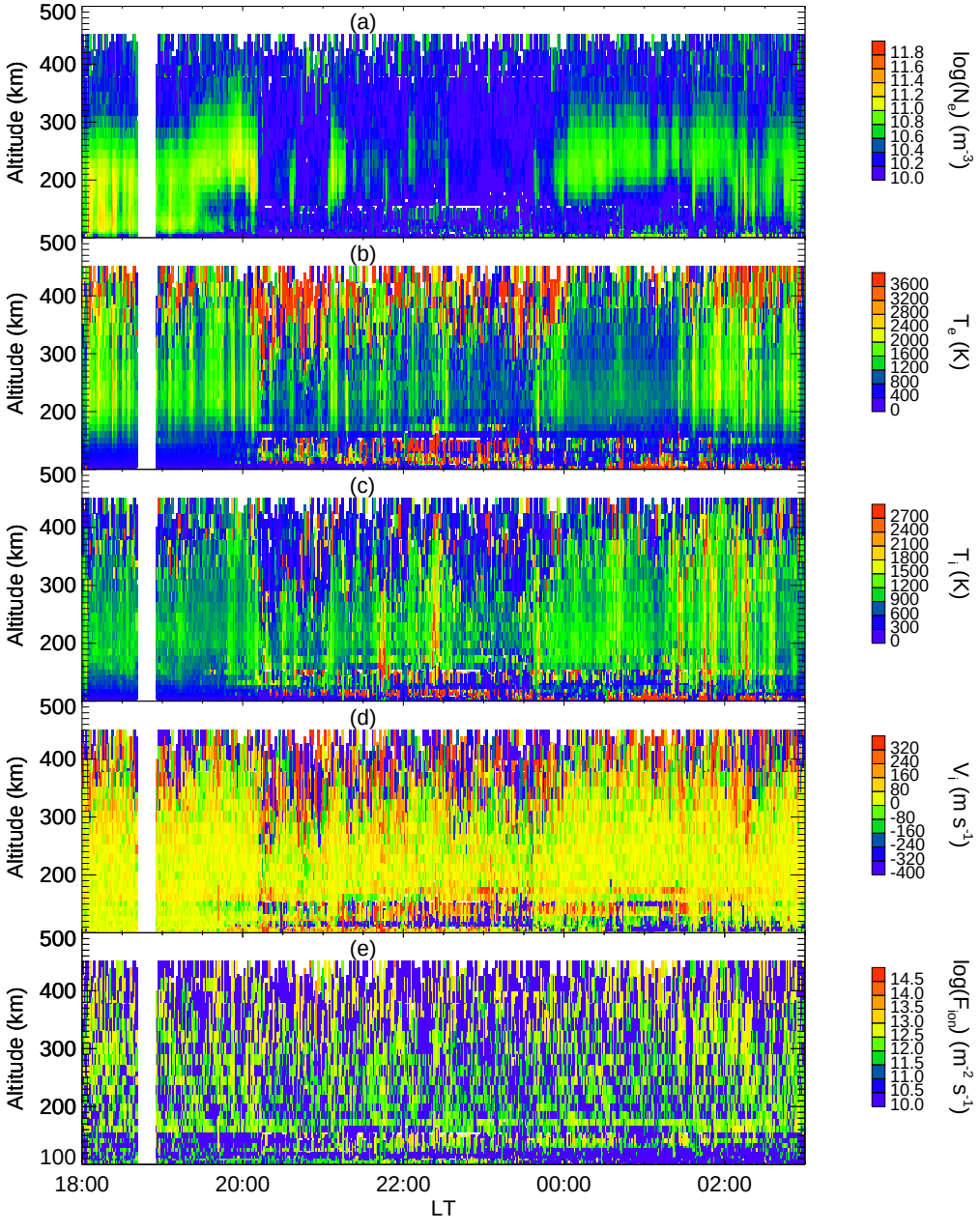

Figure 3. EISCAT Svalbard Radar (42 m dish) parameter plot for nightside 28 December, 2007. The panels a – e are respectively the electron density, electron temperature, ion temperature, ion drift velocity and the ion flux.

https://doi.org/10.5194/angeo-2023-37
Preprint. Discussion started: 4 January 2024

Annales Geophysicae Discussions
Open Access
EGU

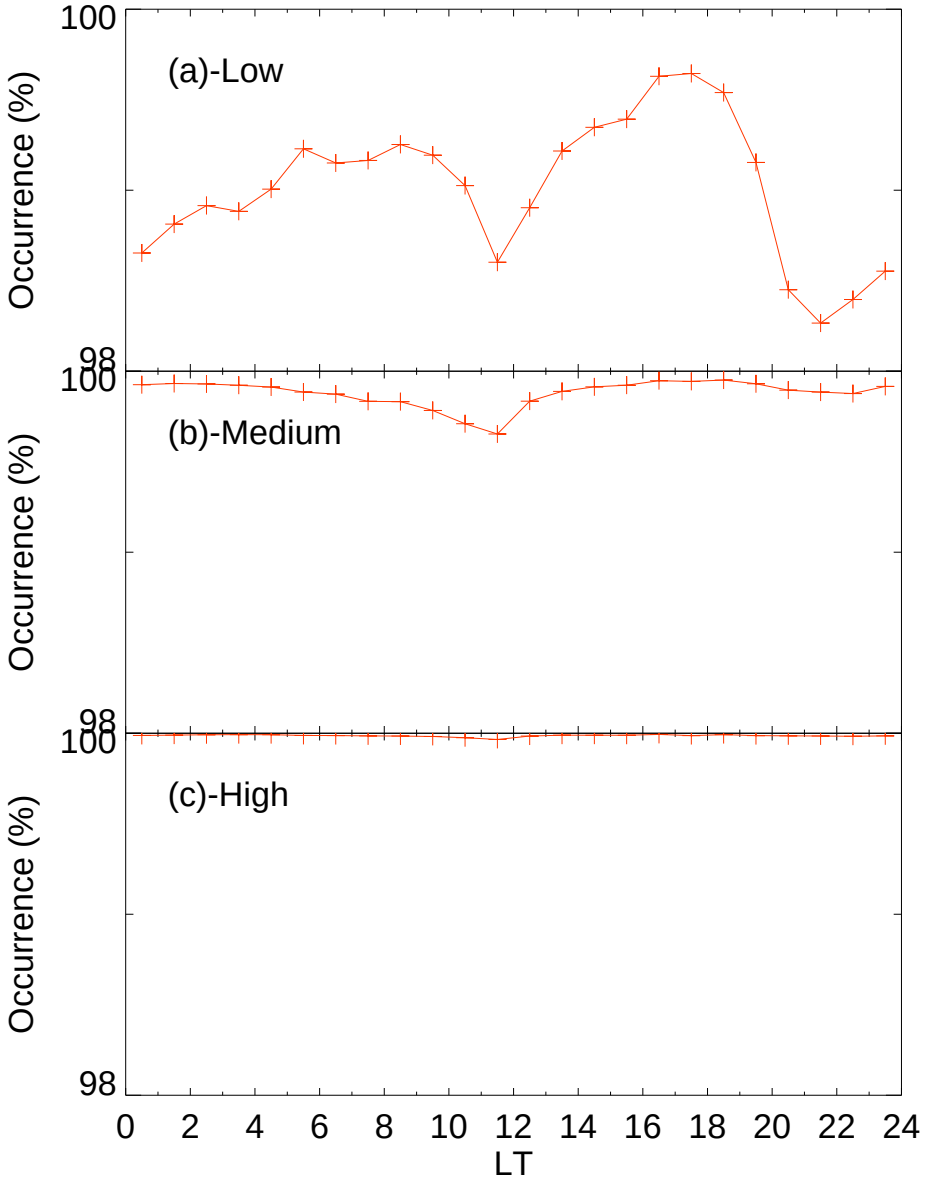

Figure 4. Local time distribution of noise occurrence in (a) low, (b) medium, and (c) high flux upflow.

(used in this work) set by David et al. (2018) for upwelling ions, while unfiltered data on the other hand is the number of data points before filtering that fell in the range of each class of upflow from the raw data obtained by the ESR during the period

https://doi.org/10.5194/angeo-2023-37
Preprint. Discussion started: 4 January 2024

Annales Geophysicae Discussions

under investigation. The percentage of the actual data is calculated from the percentage ratio of the actual to the unfiltered data points. On the other hand, percentage noise for each class is obtained by

$$noise = \left(1 - \frac{actual\ data\ point\ for\ each\ class}{unfiltered\ data\ point\ for\ each\ class}\right)$$

The low-flux upflow is a common event and analysis of filtered data reveals that its frequency is about 8 and 73 times the medium- and high-flux upflow events, respectively. The data in Table 1 indicates that about 33% of the ESR data satisfies the filter, of which about 29% contribution is from the low-flux upflow, while medium- and high-flux upflow contribute about 3.4% and 0.4% respectively. Investigation shows that the levels of noise in the three classes of upflow are about 62%, 80% and 93% for the respective low-, medium-, and high-flux upflows. It is well known that ISR data are entangled in noise, the high level occurrence observed here may be attributed to deep solar minimum around the period (David et al., 2018). It is therefore left opened to research to investigate whether data outside the solar minimum would have a lower rejection rate.

The geographical location of the ESR reported by David et al. (2018) subjects it to variable radiation flux from the Sun and a variable rate of ionisation across the seasons. The result from Table 2, under the column for actual data/noise heading, reveals that the percentage of rejected data increases from low-flux upflow to high-flux upflow irrespective of the season. The noise level in the low-flux upflow ranges from 48 – 80% across the season, whereas the medium- and high-flux upflow respectively as 68 – 87% and 87 – 95%. However, there is no any definite pattern across the season for the upflow classes. Moreover the noise level for each category of upflow is predominantly during winter and this is not unconnected with the radar data being usually of lower quality at winter. The noise as expected is minimal in summer, with a notable result as seen in the low-flux showing occurrence of actual data is about 51.6% while noise is approximately 48.4% – the only case in which actual data is above noise. Further analysis as shown in Figure 4 reveals the distribution of the three classes of ion flux upflows with respect to local time interval. The first panel of Figure 4 shows the local time variation of the noise for the low-flux upflow, where a clear trough is observed around local noon and pre-midnight. The peak of the period when noisy data is observed is shown to be between 17 – 18 LT. The minimum percentage of the noise level across LT is above 98. The middle panel of Figure 4 also indicates that the noise level for the medium-flux, though very high (above 99% across LT), is least around local noon. However, no distinct minimum is observed in the high-flux upflow shown on the last panel of Figure 4, in fact, the noisy data for the class approaches 100% for all local time.

In general, it appears that high level of rejected data is evident in ISR data and as a result, robust and stringent filtering techniques must be ensured when analysing incoherent radar data in order not to bias the result. Ogawa et al. (2009) and Endo et al. (2000) have pointed out that radar data are noisy in the topside ionosphere as a result of unphysical velocity inadvertently obtained coupled with thermal noise from receivers as well as uncertainties arising from fitting line-of sight velocity.

3 Summary and Conclusions

Noise associated with Incoherent Scatter radar (ISR) data located at Longyearbyen in Svalbard has been investigated during the solar minimum and the results are summarised thus:

https://doi.org/10.5194/angeo-2023-37
Preprint. Discussion started: 4 January 2024


Annales Geophysicae Discussions

- About 33% of the raw data satisfies the filter, of which about 29% contribution is from the low-flux upflow, while medium- and high-flux upflow contribute about 3.4% and 0.4% respectively.
- Investigation shows that the levels of noise in the three classes of upflow are about 62%, 80% and 93% for the respective low-, medium-, and high-flux upflows.
- The percentage occurrence of the noise level in the data increases with increasing flux strength, irrespective of the season.
- The noise level for each category of upflow is predominantly during winter and minimal in summer.
- A notable result as seen in the low-flux during summer shows occurrence of actual data is about 51.6% while noise is approximately 48.4% – the only case in which actual data exceeds noise.
- Local time variation indicates that the noise level peaked around 17 – 18 LT and minimum around local noon.

Data availability. The data used in this paper can be obtained via the schedule pages of the EISCAT website (https://www.eiscat.se/) and the Madrigal database.

Author contributions. TWD; conceptualisation, methodology, formal analysis, writing-original draft, project administration, C.M.M; methodology, writing-review and editing, validation, project administration, DMW; Conceptualization, supervision, resources, ATT; writing-review and editing, project administration, AEA; writing-review and editing, project administration. All authors have read and agreed to the published version of the manuscript.

Competing interests. The authors declare no conflict of interest.

Acknowledgements. The authors show their appreciation to the EISCAT Scientific Association for easy accessibility to the Madrigal database. The international community is equal applauded for the 2007 international polar year campaign that generated such high level of robust data. Great thanks to Tertiary Education Trust Fund (TETFund) of Nigeria and the Olabisi Onabanjo University, Ago-Iwoye, Nigeria, for sponsoring this research. The University of Leicester, United Kingdom, is acknowledged for allowing the use of UoL Spectre in the analysis.

https://doi.org/10.5194/angeo-2023-37
Preprint. Discussion started: 4 January 2024

Annales Geophysicae Discussions
Open Access
EGU

References

Alcayde, D.: Incoherent scatter: theory, practice and science, EISCAT Scientific Association, 1997.

Blelly, P., Robineau, A., and Alcaydé, D.: Numerical modelling of intermittent ion outflow events above EISCAT, Journal of Atmospheric and Terrestrial Physics, 58, 273–285, 1996.

David, T., Wright, D., Milan, S., Cowley, S., Davies, J., and McCrea, I.: A study of observations of ionospheric upwelling made by the EISCAT Svalbard Radar during the International Polar Year campaign of 2007, Journal of Geophysical Research: Space Physics, 123, 2192–2203, 2018.

Dougherty, J. P. and Farley, D. T.: A theory of incoherent scattering of radio waves by a plasma, Proceedings of the Royal Society of London. Series A. Mathematical and Physical Sciences, 259, 79–99, 1961.

Endo, M., Fujii, R., Ogawa, Y., Buchert, S., Nozawa, S., Watanabe, S., and Yoshida, N.: Ion upflow and downflow at the topside ionosphere observed by the EISCAT VHF radar, Annales Geophysicae, 18, 170–181, 2000.

Evans, J. V.: Theory and practice of ionosphere study by Thomson scatter radar, Proceedings of the IEEE, 57, 496–530, 1969.

Foster, C., Lester, M., and Davies, J.: A statistical study of diurnal, seasonal and solar cycle variations of F-region and topside auroral upflows observed by EISCAT between 1984 and 1996, Annales Geophysicae, 16, 1144–1158, 1998.

Fu, H., Scales, W. A., Bernhardt, P. A., Briczinski, S. J., Kosch, M. J., Senior, A., Rietveld, M. T., Yeoman, T. K., and Ruohoniemi, J. M.: Stimulated Brillouin scattering during electron gyro-harmonic heating at EISCAT, Annales geophysicae, 33, 983–990, 2015.

Gordon, W. E.: Incoherent scattering of radio waves by free electrons with applications to space exploration by radar, Proceedings of the IRE, 46, 1824–1829, 1958.

Jones, G., Williams, P., Winser, K., Lockwood, M., and Suvanto, K.: Large plasma velocities along the magnetic field line in the auroral zone, Nature, 336, 231–232, 1988.

Li, L., Ji, H.-B., and Jiang, L.: Incoherent scatter radar: High-speed signal acquisition and processing, in: 2012 IEEE International Symposium on Industrial Electronics, pp. 1136–1140, IEEE, 2012.

Ogawa, Y., Buchert, S. C., Fujii, R., Nozawa, S., and van Eyken, A.: Characteristics of ion upflow and downflow observed with the European Incoherent Scatter Svalbard radar, Journal of Geophysical Research: Space Physics, 114, 2009.

Rishbeth, H.: EISCAT: Coherence from incoherence, Nature, 313, 431–432, 1985.

Rishbeth, H. and Williams, P.: The EISCAT ionospheric radar-The system and its early results, Royal Astronomical Society, Quarterly Journal (ISSN 0035-8738), vol. 26, Dec. 1985, p. 478-512., 26, 478–512, 1985.

Skjæveland, Å., Moen, J., and Carlson, H. C.: Which cusp upflow events can possibly turn into outflows?, Journal of Geophysical Research: Space Physics, 119, 6876–6890, 2014.

Takada, M., Seki, K., Ogawa, Y., Keika, K., Kasahara, S., Yokota, S., Hori, T., Asamura, K., Miyoshi, Y., and Shinohara, I.: Low-Altitude Ion Upflow Observed by EISCAT and its Effects on Supply of Molecular Ions in the Ring Current Detected by Arase (ERG), Journal of Geophysical Research: Space Physics, 126, e2020JA028 951, 2021.

Vlasov, A., Kauristie, K., Van de Kamp, M., Luntama, J.-P., and Pogoreltsev, A.: A study of traveling ionospheric disturbances and atmospheric gravity waves using EISCAT Svalbard Radar IPY-data, Annales Geophysicae, 29, 2101–2116, 2011.

Wahlund, J.-E. and Opgenoorth, H.: EISCAT observations of strong ion outflows from the F-region ionosphere during auroral activity: Preliminary results, Geophysical Research Letters, 16, 727–730, 1989.

https://doi.org/10.5194/angeo-2023-37
Preprint. Discussion started: 4 January 2024

Annales Geophysicae Discussions
Open Access
EGU

160 Wannberg, G., Wolf, I., Vanhainen, L.-G., Koskenniemi, K., Röttger, J., Postila, M., Markkanen, J., Jacobsen, R., Stenberg, A., Larsen, R., et al.: The EISCAT Svalbard radar: A case study in modern incoherent scatter radar system design, Radio Science, 32, 2283–2307, 1997.

Williams, P.: A multi-antenna capability for the EISCAT Svalbard radar, Journal of geomagnetism and geoelectricity, 47, 685–698, 1995.

Winser, K., Jones, G., and Williams, P.: Large field-aligned velocities observed by EISCAT, Journal of Atmospheric and Terrestrial Physics, 50, 379–382, 1988.

https://doi.org/10.5194/angeo-2023-37
Preprint. Discussion started: 4 January 2024

Annales Geophysicae Discussions
Open Access
EGU

Table 1. Ion flux classification with associated signal and noise ratio.

Ion Flux	Unfiltered data point	Actual data point	Actual data (%)	Noise (%)
Low	219772	82852	37.70	62.30
Medium	49650	9810	19.76	80.24
High	16018	1131	7.06	92.94

https://doi.org/10.5194/angeo-2023-37
Preprint. Discussion started: 4 January 2024

Annales Geophysicae Discussions
Open Access
EGU

Table 2. Seasonal variation of the signal and noise ratio for different classes of ion flux upflow.

Ion Flux	Number of unfiltered data **Number of actual (filtered) data**				Accepted data (%) **Rejected data (%)**			
	spring	summer	autumn	winter	spring	summer	autumn	winter
Low	69847 (**23651**)	75154 (**38754**)	30619 (**11549**)	44152 (**8898**)	33.86 (**66.14**)	51.57 (**48.43**)	37.72 (**62.28**)	20.15 (**79.85**)
Medium	13180 (**2794**)	7583 (**2411**)	7382 (**1640**)	21505 (**2965**)	21.20 (**78.80**)	31.79 (**68.21**)	22.22 (**77.78**)	13.79 (**86.21**)
High	2665 (**171**)	1866 (**225**)	2196 (**122**)	9291 (**613**)	6.42 (**93.58**)	12.06 (**87.94**)	5.56 (**94.44**)	6.60 (**93.40**)